The Thai Journal of Veterinary Medicine

Volume 54
Issue 3 *July - September*

Article 7

November 2024

Tissue Proteomics of Feline Mammary Carcinoma: Identification of Potential Biomarkers Based on Metastatic Status and Histopathological Characteristics

Weejarin Paphussaro
Chulalongkorn University, weejarin@gmail.com

Sittiruk Roytrakul
National Science and Technology Development Agency, sittiruk@biotec.or.th

Narumon Phaonakrop
National Science and Technology Development Agency, narumon.pha@biotec.or.th

Sawanya Charoenlappanit
National Center for Genetic Engineering and Biotechnology, National Science and Technology Development Agency, sawanya.cha@ncr.nstda.or.th

Anudep Rungsipipat
Chulalongkorn University, anudep.r@chula.ac.th

Recommended Citation

Paphussaro, Weejarin; Roytrakul, Sittiruk; Phaonakrop, Narumon; Charoenlappanit, Sawanya; Rungsipipat, Anudep; Tharasanit, Theerawat; and Suriyaphol, Gunnaporn Assoc. Prof. (2024) "Tissue Proteomics of Feline Mammary Carcinoma: Identification of Potential Biomarkers Based on Metastatic Status and Histopathological Characteristics," *The Thai Journal of Veterinary Medicine*: Vol. 54: Iss. 3, Article 7.
DOI: https://doi.org/10.56808/2985-1130.3757
Available at: https://digital.car.chula.ac.th/tjvm/vol54/iss3/7

Tissue Proteomics of Feline Mammary Carcinoma: Identification of Potential Biomarkers Based on Metastatic Status and Histopathological Characteristics

Authors

Weejarin Paphussaro, Sittiruk Roytrakul, Narumon Phaonakrop, Sawanya Charoenlappanit, Anudep Rungsipipat, Theerawat Tharasanit, and Gunnaporn Suriyaphol Assoc. Prof.

Original Article

Tissue Proteomics of Feline Mammary Carcinoma: Identification of Potential Biomarkers Based on Metastatic Status and Histopathological Characteristics

Weejarin Paphussaro[1] Sittiruk Roytrakul[2] Narumon Phaonakrop[2] Sawanya Charoenlappanit[2] Anudep Rungsipipat[1] Theerawat Tharasanit[1] Gunnaporn Suriyaphol[1*]

Abstract

Feline mammary carcinoma (FMC) is a prevalent and aggressive cancer with high metastatic potential. Few tissue biomarkers have been reported to help evaluate disease progression in FMC. This study aimed to analyze the tissue proteomic profiles of metastatic feline mammary carcinoma (mFMC) and non-metastatic FMC (NmFMC) across various histological grades (HGs) and histological types (HTs) using liquid chromatography-tandem mass spectrometry (LC-MS/MS). Tissue samples were collected from 13 NmFMC, 26 mFMC, and 13 healthy controls (CTRL). Samples were trypsinized and subjected to LC-MS/MS. Proteome results were analyzed based on the metastatic status, HGs, and HTs of the samples. The findings revealed a total of 16,897 expressed proteins were identified. Among these, upregulations of interleukin 18 receptor 1 (IL18R1) and rRNA adenine N(6)-methyltransferase (DIMT1) were commonly observed in all mFMC, HG III and solid HT groups, whereas immunoglobulin heavy chain variable (IGHV), phenylalanine-tRNA ligase (FARS2) and gasdermin C (GSDMC) were markedly increased in mFMC and solid HT groups, compared with NmFMC and CTRL. Notably, H1.5 linker histone, cluster member (H1.5) expression showed a significant difference between mFMC and NmFMC in Kaplan–Meier survival analysis ($P < 0.01$). Conversely, the tumor suppressor, NOP14 nucleolar protein (NOP14), and sodium channel protein (SCN8A) were downregulated in mFMC, HG III, and solid HT groups ($P < 0.01$). In summary, this study identified potential tumor markers and tumor suppressor candidates for FMC using LC-MS/MS. Further exploration is needed to evaluate the feasibility of utilizing these protein markers in a clinical setting with a larger cohort.

Keywords: feline mammary carcinoma, histological grades, histological types, LC-MS/MS, metastasis, proteomic biomarkers

[1]*Chulalongkorn University*
[2]*National Center for Genetic Engineering and Biotechnology, National Science and Technology Development Agency*
****Correspondence**: gunnaporn.v@chula.ac.th* (G. Suriyaphol)
Received August 27, 2024
Accepted September 8, 2024

Introduction

Feline mammary gland carcinoma (FMC) is a common tumor in female cats (Giménez *et al.,* 2010; Sorenmo *et al.,* 2020). High mortality rates are frequently found in FMC due to metastasis to other visceral organs, particularly the lungs (De Campos *et al.,* 2015; Soares *et al.,* 2016a). Hence, early detection and rapid treatment are important to prolong survival rates. The standard diagnostic procedures for mammary tumors include physical examination and tissue biopsy to investigate clinical stages, histological grades (HGs), and histological types (HTs) (Giménez *et al.,* 2010). Previous studies have shown that HG I was found in non-ulcerated tubulopapillary or complex lesions, whereas large, ulcerated, solid, and micropapillary carcinomas were associated with high-grade HG and solid HT (Seixas *et al.,* 2011). In the context of biomarkers, proliferation tumor markers (HER2 and Ki-67), hormone receptors (estrogen receptor (ER) and progesterone receptor (PR)) and angiogenic markers (cyclooxygenase-2 (COX-2) and vascular endothelial growth factor (VEGF)) have been previously reported to characterize the HGs and HTs of FMC (De Campos *et al.,* 2015). Another study indicated significantly increased levels of matrix metalloproteinase-9 (MMP-9) in feline tubulopapillary carcinomas compared with controls (CTRL) (Akkoc *et al.,* 2012). HER2 is a poor prognostic biomarker in human breast cancer (Figueroa-Magalhães *et al.,* 2014). However, in the case of FMC, HER2 expression is inconsistent. High levels of HER2 expression in tissue were shown to be associated with less aggressive outcomes such as a low Ki-67 index, absence of tumoral necrosis, and lower disease stages. Additionally, no significant association between HER2 and other clinicopathological features, including histological grades and types, was documented in FMC (De Campos *et al.,* 2015; Soares *et al.,* 2016a, b). Exploration of suitable tumor biomarkers serving as metastatic and histopathological candidates is required for FMC.

Proteomics is a large-scale evaluation of proteins (Aebersold and Mann, 2003). Liquid chromatography-tandem *mass spectrometry* (*LC-MS/MS)* has been proven to be a crucial tool for investigating potential novel tissue proteomic biomarkers in several cancers, such as human ductal carcinoma *in situ* (DCIS) and invasive carcinoma as well as in canine oral melanoma and oral benign tumors (Song *et al.,* 2012; Pisamai *et al.,* 2018). In metastatic canine mammary tumors, proteomics identified several potential protein biomarkers, such as proliferating cell nuclear antigen and ferritin light chain (Klopfleisch *et al.,* 2010).

The objective of the present study was to identify tissue proteomic candidates for cats with mFMC and NmFMC across various histological types and grades using LC-MS/MS.

Materials and Methods

Sample collection and preparation: The tumor tissue samples were collected after surgical resection at the Department of Obstetrics Gynaecology and Reproduction, Small Animal Teaching Hospital, Faculty of Veterinary Science, Chulalongkorn University. For the evaluation of distant metastasis, thoracic radiographs, including ventrodorsal and lateral views, were performed. Samples were divided into 13 NmFMC samples with no lymph node or distant metastases and 26 mFMC samples with lymph node and/or distant metastases. Tissue samples were dissected for histopathological grade, histopathological type, and proteomic analyses. For the histopathological study, samples were immersion-fixed in 10% neutral buffered formalin for 24 h with standard tissue processing and paraffin embedding. According to Mills *et al.* (2014), the histological grades of FMC, based on lymphovascular invasion (0, absent; 1, present), the percentage of nuclei with abnormal nuclear form (0, ≤5% abnormal; 1, >5% abnormal) and mitotic count (0, ≤62; 1, >62), were divided into 3 grades with total scores of 0, 1, 2 and 3, representing grade 1 (low-grade carcinoma), grade 2 (intermediate-grade carcinoma) and grade 3 (high-grade carcinoma), respectively (Mills *et al.,* 2014).

For proteomic analysis, samples were kept in RNALater solution (Thermo Fisher Scientific, Waltham, MA) overnight at 4°C and stored at −20°C until analysis. Thirteen normal mammary tissue samples were collected from freshly necropsied carcasses from the Department of Pathology, Small Animal Hospital, Faculty of Veterinary Science, Chulalongkorn University. The samples were obtained with the owners' consent, and the sample collection process was approved by the Chulalongkorn University Animal Care and Use Committee (CU-ACUC) (Approval number 1831091). Approximately 100 mg of tissue was ground with liquid nitrogen and 0.5 % sodium dodecyl sulfate (SDS). After incubation for 1 h at room temperature, samples were centrifuged at 12,000 rpm for 15 min. Supernatants were kept at –20°C until analysis. Protein concentrations were determined by Modified Lowry's assay (Thermo Fisher Scientific, Waltham, MA, US) (Waterborg, 2009). Samples with a concentration of 0.1 µg/µL were mixed with 10 mM dithiothreitol (DTT) in 10 mM ammonium bicarbonate, followed by adding 100 mM iodoacetamide in 10 mM ammonium bicarbonate. Ten nanograms of trypsin in 50% acetonitrile in 10 mM ammonium bicarbonate were added. Samples were stored in 10% formic acid at –20°C until LC-MS/MS analysis.

LC-MS/MS analysis and data processing: Peptide separation was performed using Acclaim PepMap nanocolumns with 75 µm diameter × 5 cm length (Thermo Fisher Scientific, Waltham, MA, USA). The nanoLC system was linked to electrospray ionization MS in positive ion mode and quadrupole ion-trap MS (Bruker Daltonics, Billerica, MA, USA). For the mobile phase, 0.1% formic acid in distilled water was defined as eluent A, and 0.1% formic acid in 80% acetonitrile in distilled water was defined as eluent B. A linear gradient of eluent B 4–70% was achieved at a flow rate of 0.3 µL/min for 20 min. Ninety percent and 4% eluent B were used for regeneration and equilibration, respectively, for 40 min per run. For peptide fragment mass spectra analysis, a scan range of 400–1500 m/z, 3 averages, and up to 5 precursor ions selected from the MS scan at 200–2800 m/z were used. CompassXport software (Bruker Daltonics) was used to convert the

LC-MS/MS results into an mzXML file. Protein quantification was performed using DeCyder MS Differential Analysis software (*GE Healthcare*, Chicago, IL, USA). PepDetect in MS mode was used for automated peptide detection, charge state assignments, and peptide ion signal intensities. MASCOT software (Matrix Science, Boston, MA, USA) was used to identify the proteins from MS/MS peptide mass values by searching against the NCBI mammal *Felis catus* database with a MASCOT score corresponding to $P < 0.05$. To annotate protein sequences, molecular functions, and biological processes, UniProtKB/Swiss-Prot entries (http://www.uniprot.org/) were used. The relationship among sample groups was exhibited using a jVenn diagram (Bardou *et al.,* 2014). A protein-protein interaction network was analyzed using the Stitch program, version 5.0 (http://stitch.embl.de/) (Szklarczyk *et al.,* 2016). Kaplan–Meier survival curves for NmFMC and mFMC cats were analyzed.

Statistical analysis: The differential protein expression in CTRL and samples with various metastatic statuses, HGs, and HTs were analyzed using the MetaboAnalyst 6.0 software (Pang *et al.,* 2021). Additionally, a partial least square discrimination analysis (PLS-DA) was performed using the same software (Pang *et al.,* 2024). Fold change analysis between groups was presented on a $\log_2$ scale. The *Shapiro-Wilk* test in R was employed for normality testing. The Mann-Whitney U test in R was utilized to determine statistical significance, with a significance level set at $P < 0.05$. GraphPad Prism version 10.2.2 software was used to analyze survival time using the Kaplan–Meier method (log-rank test).

Table 1 Sample description data including age, breed, neuter status, metastatic status, histological grade, and histological type.

Sample ID	Age (years)	Breed	Neuter status	Metastasis	Histological grade	Histological type
1	9	DSH	-	mFMC	II	SC
2	17	DSH	-	NmFMC	II	SC
3	10	DSH	-	NmFMC	III	SC
4	5	Khao Manee	+	mFMC	II	TA
5	11	DSH	+	NmFMC	II	TA
6	12	DSH	+	mFMC	III	SC
8	8	DSH	-	NmFMC	III	SC
9	10	DSH	+	mFMC	II	TA
10	9	DSH	+	mFMC	II	TA
11	13	DSH	+	mFMC	II	TA
12	10	DSH	N/D	NmFMC	II	TA
14	7	DSH	+	NmFMC	I	TA
15	12	DSH	+	mFMC	I	TA
16	11	DSH	-	mFMC	II	TA
17	13	DSH	+	mFMC	III	SC
18	15	DSH	+	mFMC	III	SC
19	8	DSH	+	NmFMC	II	CC
20	15	DSH	-	mFMC	II	TA
21	8	DSH	+	mFMC	II	TA
23	9	Persia	-	mFMC	III	SC
24	16	DSH	-	mFMC	II	TA
26	10	Persia	+	mFMC	II	SC
28	10	DSH	+	mFMC	II	TA
29	14	DSH	+	mFMC	III	CC
30	7	DSH	+	NmFMC	I	TA
31	10	DSH	+	mFMC	II	TA
32	10	DSH	+	mFMC	II	TA
33	15	DSH	+	mFMC	II	SC
34	15	DSH	+	mFMC	II	TA
35	13	DSH	+	mFMC	I	TA
36	15	DSH	+	NmFMC	II	TA
37	N/D	DSH	+	mFMC	II	TPA
39	5	DSH	N/D	NmFMC	II	TA
40	8	DSH	N/D	NmFMC	I	TA
41	2	DSH	-	mFMC	II	DA
43	16	Persia	-	mFMC	II	TA
45	17	DSH	+	mFMC	II	SC
47	7	SH	+	NmFMC	II	CC
49	3	Persia	+	NmFMC	II	TA

Abbreviations: CC, cribriform carcinoma; DA, ductal adenocarcinoma; DSH, domestic shorthair; mFMC, metastatic feline mammary carcinoma; N/D, Not determined; NmFMC, Non-metastatic feline mammary carcinoma; SC, solid carcinoma; TA, tubular adenocarcinoma; TPA, tubulopapillary adenocarcinoma

Result

Sample description data: From 39 FMC samples, 67% were mFMC (26/39), and 33% were NmFMC (13/39). For HG classification, 69% were HG II (27/39), followed by HG III at 18% (7/39) and HG I at 13% (5/39). According to HTs, 61% were tubular adenocarcinoma (24/39), followed by 28% solid carcinoma (11/39), 8% cribriform carcinoma (3/39), and 3% ductal adenocarcinoma (1/39) (Table 1, Supplementary Fig. 2).

Proteomics results: There were 16,897 proteins expressed in this study. We found 220 proteins differentially expressed between mFMC and/or NmFMC groups compared with the CTRL group ($P < 0.01$), whereas 206 proteins were found to be differentially expressed between HG I, HG II, or HG III groups and the CTRL group ($P < 0.01$). Furthermore, a total of 275 proteins were differentially expressed between tubular adenocarcinoma, tubulopapillary carcinoma, ductal adenocarcinoma, cribriform carcinoma, or solid carcinoma groups and the CTRL group ($P < 0.01$). Among all differentially expressed proteins compared with the CTRL group, 96 proteins were commonly expressed across various metastatic statuses, HG, and HT groups (Fig. 1, Supplementary Table 1). Within this subset, interleukin 18 receptor 1 (IL18R1), rRNA adenine N(6)-methyltransferase (DIMT1), and odontogenesis-associated phosphoprotein (ODAPH) exhibited significant upregulation in mFMC, HG III, and solid HT cases compared with NmFMC and CTRL groups ($P < 0.01$) as shown in Table 2 and PLS-DA plots (Fig. 2). Apart from this, immunoglobulin heavy chain variable (IGHV), phenylalanine-tRNA ligase (FARS2), gasdermin C (GSDMC) and actinin alpha 4 (ACTN4) were markedly found in mFMC and solid HT groups compared with NmFMC and CTRL ($P < 0.01$), with the involvement of DIMT1, FARS2 and ACTN4 in the network of protein-protein interaction (Table 2, Fig. 2, Supplementary Fig. 3). Additionally, several proteins were overexpressed in both mFMC and NmFMC, as well as in solid HT and HG III compared with CTRL and HG I ($P < 0.01$), such as H1.5 ($P < 0.01$) (Table 2). In the context of HGs and HTs, 19 proteins within this subset were commonly expressed between HG and HT groups. Increased levels of transmembrane serine protease 9 (TMPRSS9) and phosphatidylinositol transfer protein cytoplasmic 1 (PITPNC1) were shown in HG III and solid carcinoma compared with CTRL and HG I ($P < 0.01$) (Fig. 1, Supplementary Table 2).

Concerning downregulated proteins, diminished levels of NOP14 nucleolar protein (NOP14) and sodium channel protein (SCN8A) were observed in mFMC, HG III, and solid HT when compared with CTRL ($P < 0.01$) (Table 2). Furthermore, several proteins were downregulated in HG III and solid HT groups compared with CTRL, including RNA helicase aquarius (AQR) and FCH and double SH3 domains 1 (FCHSD1) ($P < 0.01$) (Supplementary Table 2).

Survival time: Kaplan–Meier survival curves for NmFMC and mFMC cats, with various protein expressions including H1.5, IL18R1, DIMT1, ODAPH, FARS2 and GSDMC were analyzed. Only the H1.5 expression showed a significant difference between mFMC and NmFMC ($P < 0.05$) (Fig. 3, Supplementary Fig. 1).

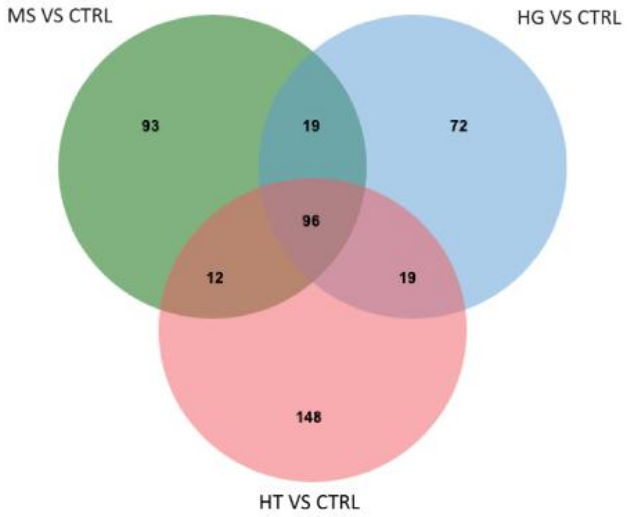

Figure 1 jVenn diagram of expressed proteins in different metastatic statuses (MS), histological grades (HG), and histological types (HT) compared with controls (CTRL).

Table 2 Differentially expressed proteins in various metastatic statuses, histological grades, and histological types based on molecular function by UniProtKB/Swiss-Prot. Fold change analysis between groups was presented on a log2 scale.

Protein name (Abbreviation)	Peptides	CTRL	mFMC	NmFMC	Histological grade			Histological type				Molecular function
					I	II	III	CC	DA	SC	TA	
Overexpressed proteins in FMC:												
Interleukin 18 receptor 1 (IL18R1)	HSITAVEGEFFYLR	4.15^{c}	13.80^{a}	11.22^{b}	5.94^{c}	13.84^{a}	14.58^{a}	14.48^{a}	0.00^{c}	14.90^{b}	12.31^{a}	hydrolase activity
rRNA adenine N(6)-methyltransferase (EC 2.1.1.-) (DIMT1)	CAVLMFQR	5.60^{c}	13.52^{a}	8.89^{b}	6.18^{c}	13.19^{a}	11.15^{a}	4.54^{c}	14.47^{a}	13.61^{a}	12.66^{a}	RNA binding, rRNA (adenine-N6,N6-)-dimethyltransferase activity
Odontogenesis-associated phosphoprotein (ODAPH)	AHQRRFACR	5.55^{c}	10.77^{a}	8.43^{b}	8.47^{b,c}	9.98^{b}	11.31^{a}	4.56^{c}	0.00^{c}	10.89^{a}	10.46^{a}	positive regulation of enamel mineralization
IgH variable region (IGHV)	APSVFPR	8.15^{c}	13.93^{a}	9.83^{c}	9.09^{c}	14.59^{a}	6.02^{c}	5.13^{c}	0.00^{c}	13.33^{a}	14.19^{a}	
Gasdermin C (GSDMC)	ASAGVTAMLETNVSGEATK	1.81^{b}	9.73^{a}	5.07^{b}	5.24^{a,b}	9.50^{a}	4.45^{a,b}	8.50	14.44	6.61^{a}	8.69^{a}	phosphatidylserine binding
Actinin alpha 4 (ACTN4)	ALDFIASK	4.80^{b}	11.46^{a}	8.76^{b}	10.45	11.42	6.65	13.90^{c}	13.56	9.09^{a}	11.06^{a,c}	actin filament binding
Phenylalanine--tRNA ligase (EC 6.1.1.20) (Phenylalanyl-tRNA synthetase) (FARS2)	DGESLQLFEQSSRSAYK	1.03^{b}	10.33^{a}	6.90^{b}	10.15	9.56^{a}	6.65	8.89^{b}	0	8.01^{b}	9.82^{b}	ATP binding, phenylalanine-tRNA ligase activity, tRNA binding
H1.5 linker histone, cluster member (H1.5)	ALAAAGYDVEK	9.07^{b}	13.39^{a}	14.23^{a}	13.19^{b}	13.43^{a}	15.21^{a}	14.92^{a}	13.85	13.90^{a}	13.32^{a}	double-stranded DNA binding, histone deacetylase binding
Decreased expressed proteins in FMC:												
NOP14 nucleolar protein (NOP14)	AQPSNRMKTQEELAK	11.69^{a}	3.65^{b}	6.34^{b}	5.58^{b}	4.90^{b}	2.05^{b}	4.28^{b}	14.37^{a}	3.63^{b}	3.86^{b}	enzyme binding
Sodium channel protein (SCN8A)	EAEFKAMLEQLK	14.49^{a}	5.09^{b}	5.22^{b}	4.80^{b}	5.37^{b}	4.30^{b}	5.07^{b}	0.00^{b}	4.02^{b}	5.78^{b}	voltage-gated ion channel activity
RNA helicase aquarius (AQR)	ASLCNLYNWR	12.79^{a}	N/A	N/A	8.26^{a}	7.34^{b}	2.00^{c}	8.31	0.00	1.22^{c}	8.91^{a}	helicase activity, RNA binding
FCH and double SH3 domains 1 (FCHSD1)	AQAEVLQSVRELSR	8.61^{a}	N/A	N/A	7.88^{a,b}	5.79^{b}	2.92^{c}	4.79^{b}	15.64^{a}	6.20^{b}	9.02^{b}	lipid binding

a, b, c, d denote a significant difference in each classification $P < 0.01$

Abbreviations: CTRL, controls CC, cribriform carcinoma; DA, ductal adenocarcinoma; mFMC, metastatic feline mammary carcinoma; N/A, not analysis; NmFMC, non-metastatic feline mammary carcinoma; SC, solid carcinoma; TA, tubular adenocarcinoma.

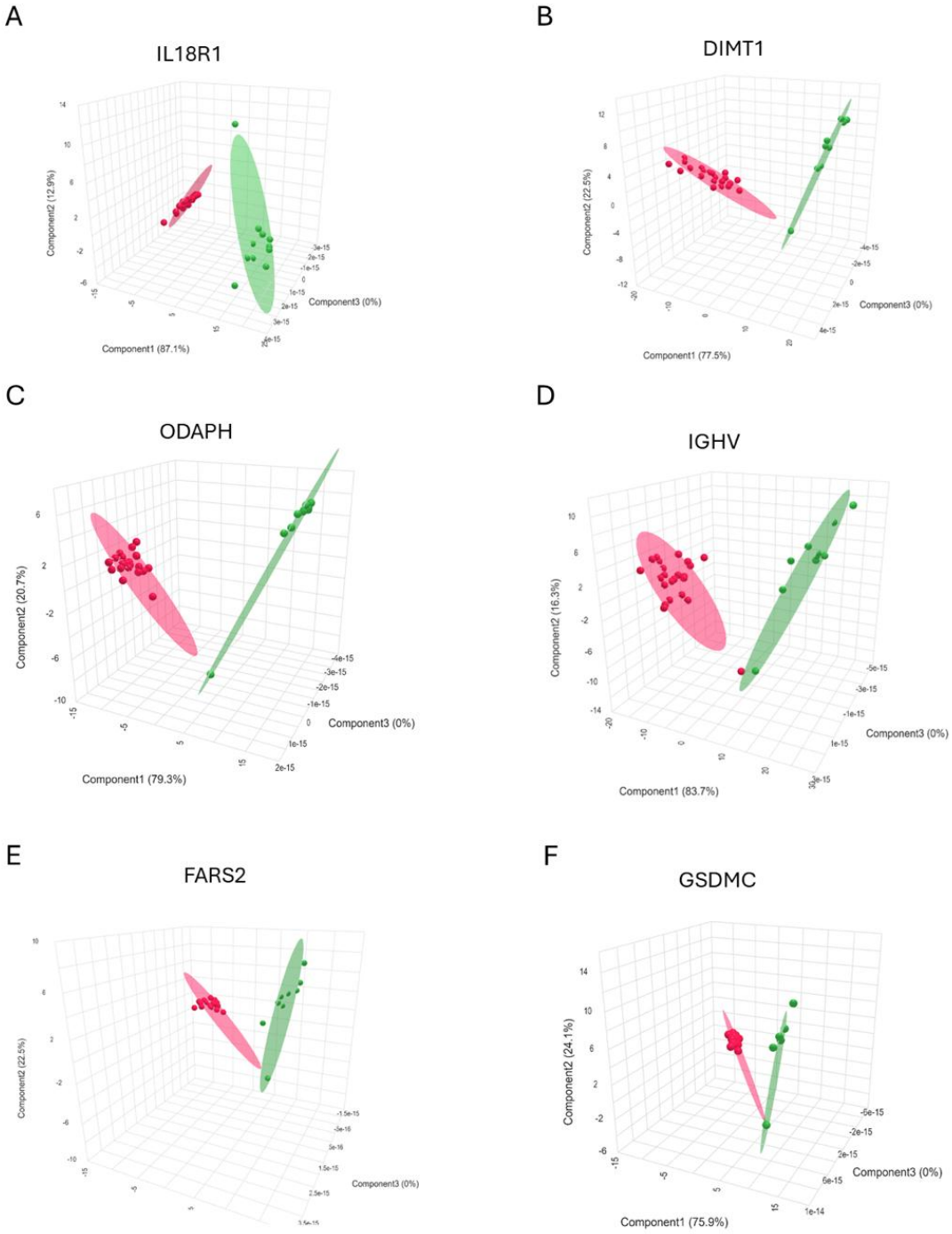

Figure 2 Partial least square discrimination analysis (PLS-DA) plot showed discriminace of mFMC and NmFMC in various proteins (red circle- mFMC, green circle- NmFMC). Interleukin 18 receptor 1 (IL18R1) (A), rRNA adenine N(6)-methyltransferase (DIMT1) (B), odontogenesis associated phosphoprotein (ODAPH) (C), immunoglobulin heavy chain variable (IGHV) (D), phenylalanine--tRNA ligase (FARS2) (E) and gasdermin C (GSDMC) (F).

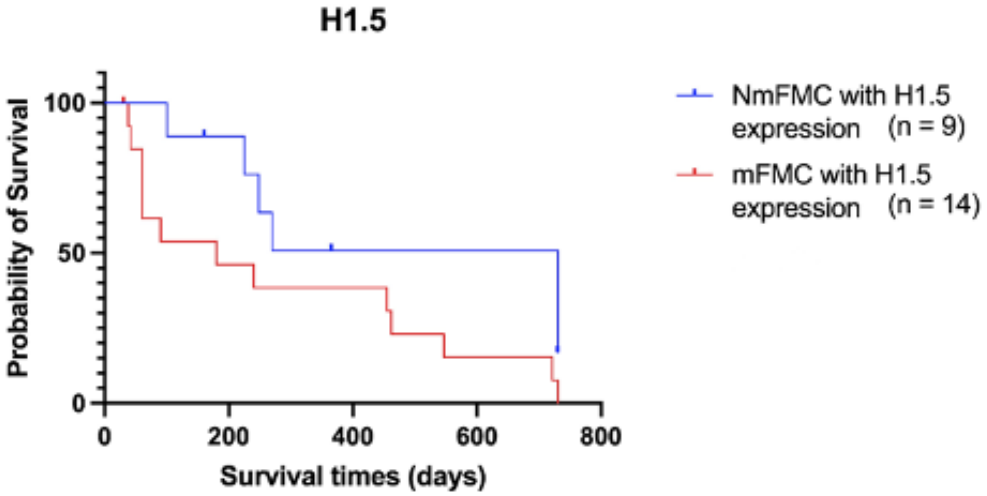

Figure 3 Kaplan–Meier survival curve for NmFMC and mFMC with H1.5 linker histone, cluster member (H1.5) expression (P = 0.0459). The tick mark indicated censored cats. ($P < 0.05$).

.

Discussion

In the present study, several novel tissue proteins with various metastatic statuses, HGs, and HTs were identified in FMC using LC-MS/MS. The first target group included proteins expressed under the most aggressive conditions (mFMC, solid HT, and HG III) compared with NmFMC and CTRL, including IL18R1, DIMT1, and ODAPH. The second target group comprised proteins observed in mFMC and solid HT compared with NmFMC and CTRL, such as IGHV, FARS2, GSDMC, and ACTN4. Within these groups, proteins could be classified into those related to immune response **(**IL18R1 and IGHV), proteins involved in cell proliferation (DIMT1, FARS2 and GSDMC) and proteins with other functions (ODAPH) (Babbage *et al.,* 2006; Tang *et al.,* 2020; Sattari *et al.,* 2021; Shen *et al.,* 2021; Ho *et al.,* 2022; Yang and Tang, 2023). IL18R1, a cytokine receptor, plays an important role in the IL-18 signaling pathway. IL18R1 was found to be overexpressed in human breast cancer tissues compared with nearby non-cancerous tissues, possibly because IL18R1 was potentially involved in immune escape, resulting in the tumorigenesis of breast cancer cells. Additionally, IL18R1 levels were increased in T cells obtained from invasive ductal carcinoma samples compared with *in situ* tumors (Tang *et al.,* 2020; Sattari *et al.,* 2021). IGHV has been reported in breast cancer cells. Immunoglobulin heavy constant alpha 2 (IGHA2) was identified in breast tumor cells that metastasized to regional lymph nodes using matrix-assisted laser desorption/ionization-mass spectrometry imaging (MALDI-MSI), immunoblotting and immunohistochemical analysis. Moreover, human breast cancer cells secreted immunoglobulin G (IgG) and supported the growth of cancer cells (Qiu *et al.,* 2003; Babbage *et al.,* 2006; Kang *et al.,* 2012).

In the context of proteins involved in cell proliferation, DIMT1 functions to promote cell proliferation in various human cancers (Shen *et al.,* 2021). High expression of DIMT1 was associated with cell proliferation and progression in multiple myeloma, thyroid cancer, and colon cancer (Shen *et al.,* 2021; Hou *et al.,* 2023). In addition, DIMT1 was overexpressed in gastric carcinoma compared with normal tissue and correlated with metastasis; however, the mechanism has not been reported (Liu *et al.,* 2017). Phenylalanyl-tRNA synthetase alpha chain (*FARSA*) gene expression was shown to be upregulated in several tumors, and its protein functions to regulate tumor cell proliferation and/or differentiation (Ho *et al.,* 2022). FARS2 was found to be increased in various human cancers (Sung *et al.,* 2022). GSDMC plays an important role in inducing the pyroptosis pathway causing tumor necrosis, and thus, high expression of GSDMC correlates with poor survival times (Hou *et al.,* 2020; Yang and Tang, 2023). Additionally, ACTN4 plays an essential role in breast cancer stem cell-related metastasis (Wang *et al.,* 2017). The expression of ODAPH was associated with thin and hypoplastic enamel in mice (Mu *et al.,* 2022). Notably, advanced-stage human breast cancer and patients undergoing chemotherapy can lead to dry mouth (xerostomia), contributing to decay and enamel erosion (Pinto *et al.,* 2020; Talha and Swarnkar, 2023; Walsh *et al.,* 2023). However, the association of ODAPH expression and enamel erosion in FMC needs to be further investigated.

Regarding the survival time analysis, only H1.5 expression was correlated with longer survival in NmFMC compared with mFMC. Histone H1.5 plays important roles in gene expression, DNA repair, and cell proliferation. This protein was targeted to differentiate prostate cancer from benign prostatic glands by immunohistochemistry (Khachaturov *et al.,* 2014). The association of other proteins (IL18R1, DIMT1, ODAPH, and FARS2) with survival rates was not observed, possibly due to the analysis of the Kaplan–Meier survival graph based on the survival time of patients after surgery only, regardless of the protein expression values.

Focusing on HG and HT groups, TMPRSS9 and PITPNC1 were found to be commonly upregulated in high-grade HG and solid HT. TMPRSS9 is a member of the type II transmembrane serine protease (TTSP) family, influencing pro-tumor activities in pancreatic cancer cells. Hence, TMPRSS9 or polymerase-1 may affect tumor progression and prevent the progression of this malignant tumor by inhibiting protein activity (Fontanil *et al.,* 2014). In breast cancer, TMPRSS2 was

found to be a potential biomarker for poor patient survival34 and as a prognostic marker correlated with immune infiltrates in breast invasive cancer (Xiao *et al.*, 2022). In the context of phosphatidylinositol transfer proteins (PITPs), they are multifunctional proteins that play an important role in signal transduction and membrane trafficking processes (Grabon *et al.*, 2015). The PITPNC1 gene was found to be overexpressed in metastatic breast, melanoma, and colon cancer (Halberg *et al.*, 2016; Cavieres *et al.*, 2020). Knockdown of PITPNC1 decreased the metastatic potential of human breast cancer cells(Png *et al.*, 2011; Halberg *et al.*, 2016).

Potential tumor suppressor markers in FMC, such as NOP14 and SCN8A, were markedly decreased in the FMC group with various metastatic statuses, HGs, and HTs compared with CTRL. Overexpression of NOP14 suppresses breast cancer metastasis via inhibition of the NRIP1/Wnt/β-catenin pathway. Moreover, low expression of NOP14 was associated with poor prognosis in breast cancer (Lei *et al.*, 2015). Decreased expression of SCN8A was observed in the tumor tissues of patients with colorectal carcinoma compared with normal tissue (Igci *et al.*, 2015). In addition, lower levels of AQR and FCHSD1 were noted in HG III and solid HT groups compared with CTRL. AQR is a pre-mRNA splicing factor and might prevent cancer by maintaining genome integrity due to repairing DNA damage during the S phase (related to the R loop) (Sakasai *et al.*, 2017). FCHSD1 and FCHSD2 could regulate F-actin assembly in hair cell stereocilia and the cuticular plate, and stabilized F-actin structure led to the limitation of migration and metastasis of cancer cells (Cao *et al.*, 2013; Izdebska *et al.*, 2020).

In summary, potential protein candidates in feline mammary carcinomas using LC-MS/MS across different metastatic statuses, HGs, and HTs of FMC were identified in this study. These included proteins markedly expressed in mFMC and high HG (HG III) related to immune response (IL18R1 and IGHV**),** cell proliferation (DIMT1, FARS2, and GSDMC), and other functions (ODAPH). Additionally, TMPRSS9 and PITPNC1 were upregulated in high-grade HG and solid HT. In contrast, potential tumor suppressors of FMC, such as NOP14, SCN8A, AQR, and FCHSD1, were identified. The limitations of this study include limited sample size, especially in the metastatic stage of FMC, due to some cats not undergoing surgery. Future research in a larger population with validation should be done to investigate the precise roles of these candidates.

Data availability: Additional data is available in the supplementary material. The raw MS/MS spectra data are available in ProteomeXchange (PXD053213) (https://proteomecentral.proteomexchange.org/cgi/GetDataset?ID=PXD053213).

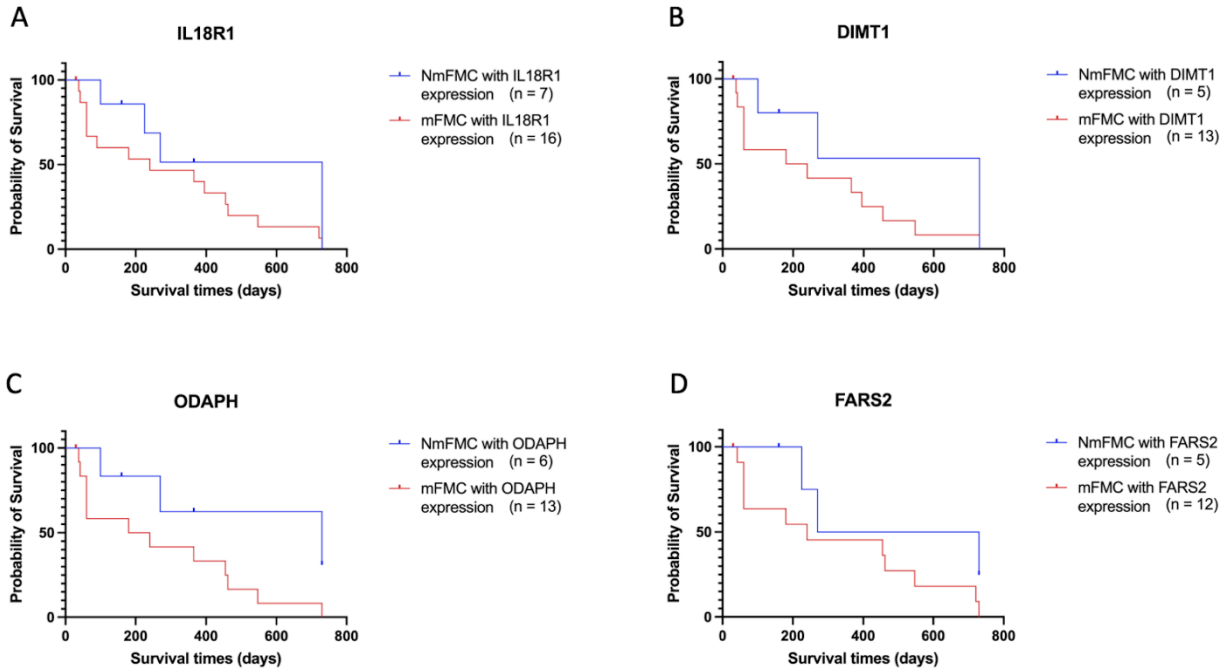

Supplementary Figure 1 Kaplan–Meier survival curve for NmFMC and mFMC cats, with interleukin 18 receptor 1 (IL18R1) ($P < 0.115$) (A), rRNA adenine N(6)-methyltransferase (DIMT1) ($P < 0.129$) (B), odontogenesis associated phosphoprotein (ODAPH) ($P < 0.056$) (C) and phenylalanine-tRNA ligase (FARS2) ($P < 0.119$) (D). The tick mark indicated censored cats.

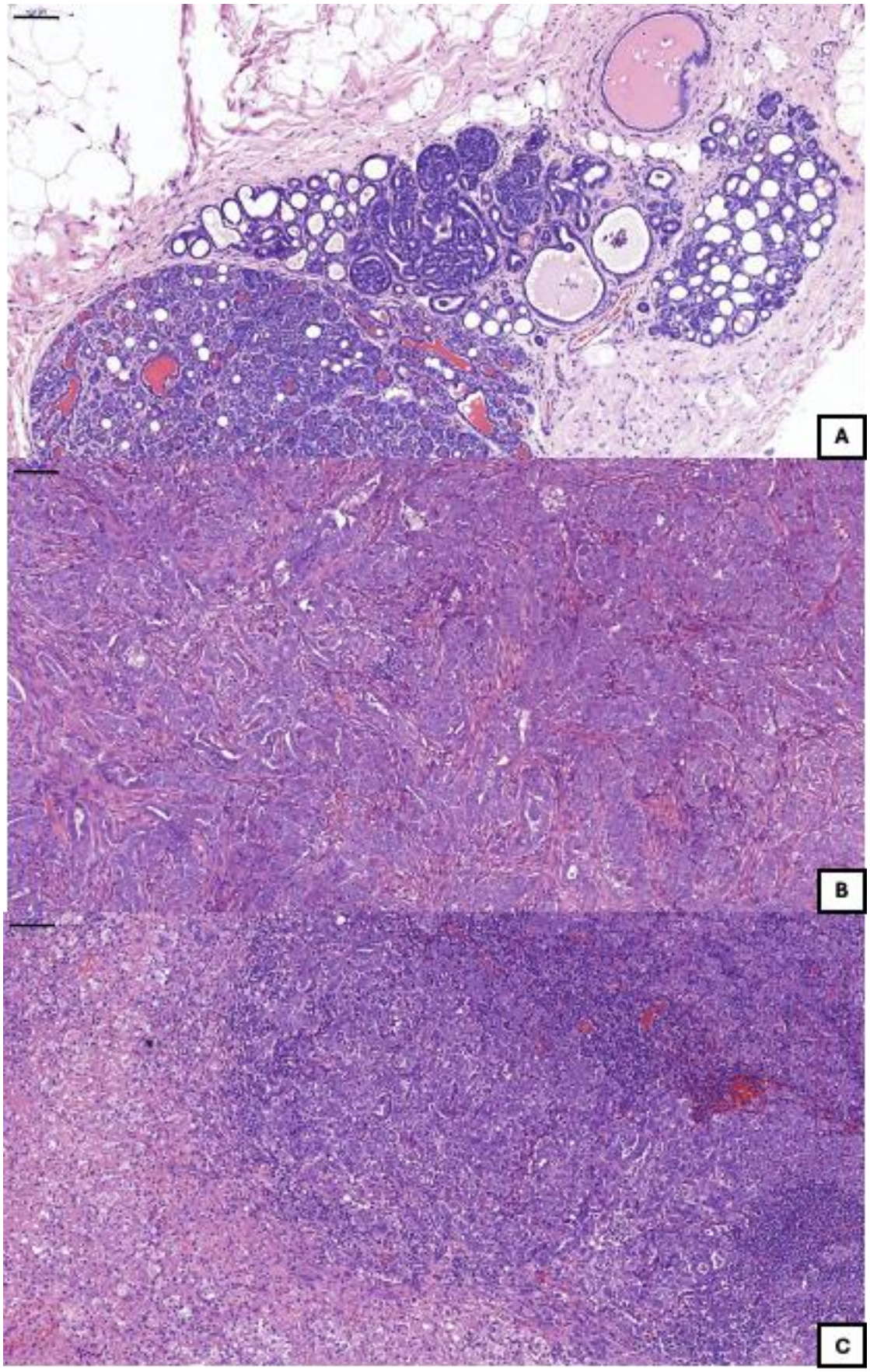

Supplementary Figure 2 Histopathological grades and types of feline mammary carcinoma. Tubular adenocarcinoma with histological grade I (A), tubular adenocarcinoma with histological grade II (B), and solid carcinoma with histological grade III (C). Scale bar = 100 μm.

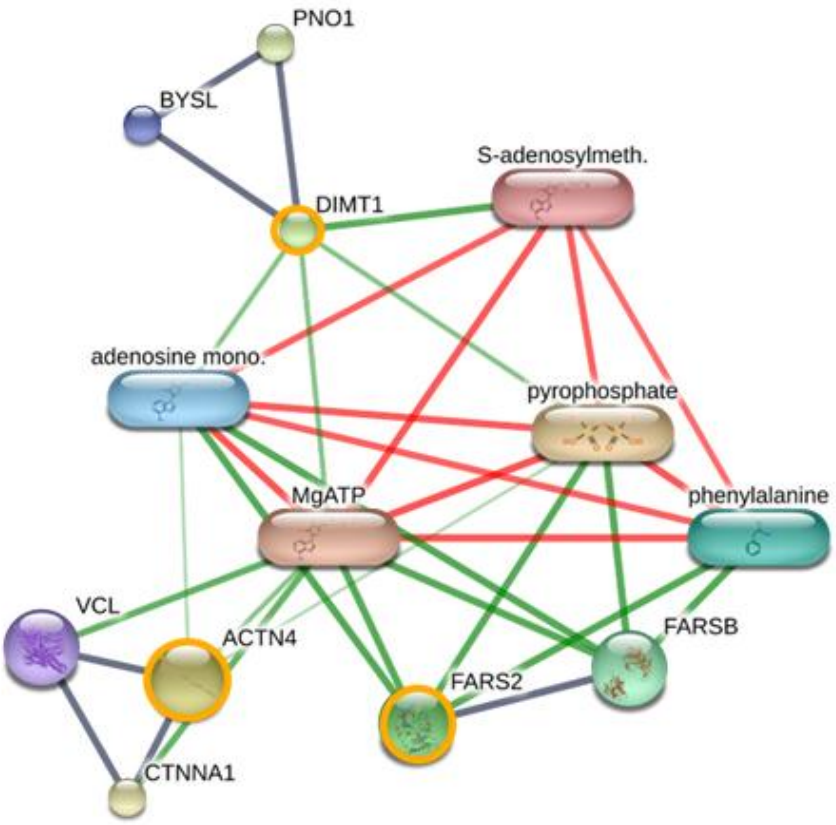

Supplementary Figure 3 A protein-protein interaction network of rRNA adenine N(6)-methyltransferase (DIMT1), phenylalanine-tRNA ligase (FARS2) and actinin alpha 4 (ACTN4). Yellow circles: DIMT1, FARS2, and ACTN4. Abbreviations: bystin (BYSL), catenin alpha 1 (CTNNA1), phenylalanyl-TRNA synthetase subunit beta (FARSB), RNA-binding protein PNO1 (PNO1), vinculin (VCL).

References

Aebersold R and Mann M 2003. Mass spectrometry-based proteomics. Nature. 422: 198–207.

Akkoc A, Inan S and Sonmez G 2012. Matrix metalloproteinase (MMP-2 and MMP-9) and steroid receptor expressions in feline mammary tumors. Biotech Histochem. 87: 312–319.

Babbage G, Ottensmeier CH, Blaydes J, Stevenson FK and Sahota SS 2006. Immunoglobulin heavy chain locus events and expression of activation-induced cytidine deaminase in epithelial breast cancer cell lines. Cancer Res. 66: 3996–4000.

Bardou P, Mariette J, Escudié F, Djemiel C and Klopp C 2014. jvenn: an interactive Venn diagram viewer. BMC Bioinformatics. 15: 293.

De Campos CB, Damasceno KA, Gamba CO, Ribeiro AM, Machado CJ, Lavalle GE and Cassali GD 2015. Evaluation of prognostic factors and survival rates in malignant feline mammary gland neoplasms. J Feline Med Surg. 18:1003–1012.

Cao H, Yin X, Cao Y, Jin Y, Wang S, Kong Y, Chen Y, Gao J, Heller S and Xu Z 2013. FCHSD1 and FCHSD2 are expressed in hair cell stereocilia and cuticular plate and regulate actin polymerization in vitro. PLoS One. 8: e56516.

Cavieres VA, Cerda-Troncoso C, Rivera-Dictter A, Castro RI, Luchsinger C, Santibañez N, Burgos PV and Mardones GA 2020. Human golgi phosphoprotein 3 is an effector of RAB1A and RAB1B. PLoS One. 15: e0237514.

Figueroa-Magalhães MC, Jelovac D, Connolly RM and Wolff AC 2014. Treatment of HER2-positive breast cancer. Breast. 23: 128–136.

Fontanil T, Mohamedi Y, Esteban MM, Obaya AJ and Cal S 2014. Polyserase-1/TMPRSS9 induces pro-tumor effects in pancreatic cancer cells by activation of pro-uPA. Oncol Rep. 31: 2792–2796.

Giménez F, Hecht S, Craig LE and Legendre AM 2010. Early detection, aggressive therapy: optimizing the management of feline mammary masses. J Feline Med Surg. 12: 214–224.

Grabon A, Khan D and Bankaitis VA 2015. Phosphatidylinositol transfer proteins and instructive regulation of lipid kinase biology. Biochim Biophys Acta. 1851: 724–735.

Halberg N, Sengelaub CA, Navrazhina K, Molina H, Uryu K and Tavazoie SF 2016. PITPNC1 recruits RAB1B to the golgi network to drive malignant secretion. Cancer Cell. 29: 339–353.

Ho MT, Lu J, Vazquez-Pianzola P and Suter B 2022. α-Phenylalanyl tRNA synthetase competes with Notch signaling through its N-terminal domain. PLoS Genetics. 18: e1010185.

Hou J, Zhao R, Xia W, Chang CW, You Y, Hsu JM, Nie L, Chen Y, Wang YC, Liu C, Wang WJ, Wu Y, Ke B, Hsu JL, Huang K, Ye Z, Yang Y, Xia X, Li Y, Li CW, Shao B, Tainer JA and Hung MC 2020. PD-L1-

mediated gasdermin C expression switches apoptosis to pyroptosis in cancer cells and facilitates tumour necrosis. Nat Cell Biol. 22: 1264–1275.

Hou X, Tian M, Ning J, Wang Z, Guo F, Zhang W, Hu L, Wei S, Hu C, Yun X, Zhao J, Dong Q, Ruan X, Li D, Gao M and Zheng X 2023. PARP inhibitor shuts down the global translation of thyroid cancer through promoting Pol II binding to DIMT1 pause. Int J Biol Sci. 19: 3970–3986.

Igci YZ, Bozgeyik E, Borazan E, Pala E, Suner A, Ulasli M, Gurses SA, Yumrutas O, Balik AA and Igci M 2015. Expression profiling of SCN8A and NDUFC2 genes in colorectal carcinoma. Exp Oncol. 37: 77–80.

Izdebska M, Zielińska W, Hałas-Wiśniewska M and Grzanka A 2020. Involvement of actin and actin-binding proteins in carcinogenesis. Cells. 9: 2245.

Kang S, Maeng H, Kim BG, Qing GM, Choi YP, Kim HY, Kim PS, Kim Y, Kim YH, Choi YD and Cho NH 2012. In situ identification and localization of IGHA2 in the breast tumor microenvironment by mass spectrometry. J Proteome Res. 11: 4567–4574.

Khachaturov V, Xiao GQ, Kinoshita Y, Unger PD and Burstein DE 2014. Histone H1.5, a novel prostatic cancer marker: an immunohistochemical study. Hum Pathol. 45: 2115–2119.

Klopfleisch R, Klose P, Weise C, Bondzio A, Multhaup G, Einspanier R and Gruber AD 2010. Proteome of metastatic canine mammary carcinomas: similarities to and differences from human breast cancer. J Proteome Res. 9: 6380–6391.

Lei JJ, Peng RJ, Kuang BH, Yuan ZY, Qin T, Liu WS, Guo YM, Han HQ, Lian YF, Deng CC, Zhang HJ, Chen LZ, Feng QS, Xu M, Feng L, Bei JX and Zeng YX 2015. NOP14 suppresses breast cancer progression by inhibiting NRIP1/Wnt/β-catenin pathway. Oncotarget. 6: 25701–25714.

Liu G, Peng X, Cai Y, Cheng A, Zha L and Wang Z 2017. DIMT1 overexpression correlates with progression and prognosis in gastric carcinoma. Hum Pathol. 70: 35–42.

Mills SW, Musil KM, Davies JL, Hendrick S, Duncan C, Jackson ML, Kidney B, Philibert H, Wobeser BK and Simko E 2014. Prognostic value of histologic grading for feline mammary carcinoma: a retrospective survival analysis. Vet Pathol. 52: 238–249.

Mu H, Dong Z, Wang Y, Chu Q, Gao Y, Wang A, Wang Y, Liu X and Gao Y 2022. Odontogenesis-associated phosphoprotein (ODAPH) overexpression in ameloblasts disrupts enamel formation via inducing abnormal mineralization of enamel in secretory stage. Calcif Tissue Int. 111: 611–621.

Ozyurt R, Kahraman N, Dundar PA and Ozpolat B 2023. Abstract 3890: TMPRSS2 serin protease is a novel biomarker for ER+ breast cancer patient prognosis and survival and mediates resistance to anti-estrogen treatment in ER+ breast cancer. Cancer Res. 83: 3890–3890.

Pang Z, Chong J, Zhou G, de Lima Morais DA, Chang L, Barrette M, Gauthier C, Jacques PÉ, Li S and Xia J 2021. MetaboAnalyst 5.0: narrowing the gap between raw spectra and functional insights. Nucleic Acids Res. 49: W388–W396.

Pang Z, Lu Y, Zhou G, Hui F, Xu L, Viau C, Spigelman AF, MacDonald PE, Wishart DS, Li S and Xia J 2024. MetaboAnalyst 6.0: towards a unified platform for metabolomics data processing, analysis and interpretation. Nucleic Acids Res. 52: W398–W406.

Pinto VL, Fustinoni SM, Nazário ACP, Facina G and Elias S 2020. Prevalence of xerostomia in women during breast cancer chemotherapy. Rev Bras Enferm. 73.

Pisamai S, Roytrakul S, Phaonakrop N, Jaresitthikunchai J and Suriyaphol G 2018. Proteomic analysis of canine oral tumor tissues using MALDI-TOF mass spectrometry and in-gel digestion coupled with mass spectrometry (GeLC MS/MS) approaches. PLoS One. 13: e0200619.

Png KJ, Halberg N, Yoshida M and Tavazoie SF 2011. A microRNA regulon that mediates endothelial recruitment and metastasis by cancer cells. Nature. 481: 190–194.

Qiu X, Zhu X, Zhang L, Mao Y, Zhang J, Hao P, Li G, Lv P, Li Z, Sun X, Wu L, Zheng J, Deng Y, Hou C, Tang P, Zhang S and Zhang Y 2003. Human epithelial cancers secrete immunoglobulin g with unidentified specificity to promote growth and survival of tumor cells. Cancer Res. 63: 6488–6495.

Sakasai R, Isono M, Wakasugi M, Hashimoto M, Sunatani Y, Matsui T, Shibata A, Matsunaga T and Iwabuchi K 2017. Aquarius is required for proper CtIP expression and homologous recombination repair. Sci Rep. 7: 13808.

Sattari A, Hussen BM, Ghafouri-Fard S, Alihashemi A, Omrani MD, Zekri A and Taheri M 2021. Expression of T helper 1-associated lncRNAs in breast cancer. Exp Mol Pathol. 119: 104619.

Szklarczyk D, Santos A, von Mering C, Jensen LJ, Bork P and Kuhn M 2016. STITCH 5: augmenting protein-chemical interaction networks with tissue and affinity data. Nucleic Acids Res. 44: D380–D384.

Seixas F, Palmeira C, Pires MA, Bento MJ and Lopes C 2011. Grade is an independent prognostic factor for feline mammary carcinomas: A clinicopathological and survival analysis. Vet J. 187: 65–71.

Shen H, Gonskikh Y, Stoute J and Liu KF 2021. Human DIMT1 generates N26,6A-dimethylation–containing small RNAs. J Biol Chem. 297: 101146.

Soares M, Correia J, Peleteiro MC and Ferreira F 2016a. St Gallen molecular subtypes in feline mammary carcinoma and paired metastases—disease progression and clinical implications from a 3-year follow-up study. Tumor Biol. 37: 4053–4064.

Soares M, Ribeiro R, Najmudin S, Gameiro A, Rodrigues R, Cardoso F and Ferreira F 2016b. Serum HER2 levels are increased in cats with mammary carcinomas and predict tissue HER2 status. Oncotarget. 7: 17314–17326.

Song MN, Moon PG, Lee JE, Na M, Kang W, Chae YS, Park JY, Park H and Baek MC 2012. Proteomic analysis of breast cancer tissues to identify biomarker candidates by gel-assisted digestion and label-free quantification methods using LC-MS/MS. Arch Pharm Res. 35: 1839–1847.

Sorenmo K, Worley DR and Zappulli V 2020. Tumors of the mammary gland. In: Withrow and MacEwen's Small Animal Clinical Oncology. DM

Vail, DH Thamm and JM Liptak (eds) 6th ed. St. Louis: Elsevier. 604–625.

Sung Y, Yoon I, Han JM and Kim S 2022. Functional and pathologic association of aminoacyl-tRNA synthetases with cancer. Exp Molec Med. 54: 553–566.

Talha B and Swarnkar S A 2023. Xerostomia. In: StatPearls [Internet]. Treasure Island (FL): StatPearls Publishing. Available: https://www.ncbi.nlm.nih.gov/books/NBK545287/. Accessed July 12, 2024.

Tang S, Ning Q, Yang L, Mo Z and Tang S 2020. Mechanisms of immune escape in the cancer immune cycle. Int Immunopharmacol. 86: 106700.

Walsh M, Fagan N and Davies A 2023. Xerostomia in patients with advanced cancer: a scoping review of clinical features and complications. BMC Palliative Care. 22: 178.

Wang N, Wang Q, Tang H, Zhang F, Zheng Y, Wang S, Zhang J, Wang Z and Xie X 2017. Direct inhibition of ACTN4 by ellagic acid limits breast cancer metastasis via regulation of β-catenin stabilization in cancer stem cells. J Exp Clin Cancer Res. 36: 172.

Waterborg JH 2009. The Lowry method for protein quantitation. In: The Protein Protocols Handbook. JM Walker (ed). New York: Humana Press. 7–10.

Xiao X, Shan H, Niu Y, Wang P, Li D, Zhang Y, Wang J, Wu Y and Jiang H 2022. TMPRSS2 serves as a prognostic biomarker and correlated with immune infiltrates in breast invasive cancer and lung adenocarcinoma. Front Mol Biosci. 9: 647826.

Yang X and Tang Z 2023. Role of gasdermin family proteins in cancers (Review). Int J Oncol. 63: 100.